https://doi.org/10.5194/hess-2020-14
Preprint. Discussion started: 23 January 2020

Hydrology and Earth System Sciences
Discussions

Vapor plumes in a tropical wet forest: spotting the invisible evaporation

César Dionisio Jiménez–Rodríguez[1,2], Miriam Coenders–Gerrits[1], Bart Schilperoort[1], Adriana Gonzalez–Angarita[3], and Hubert Savenije[1]

[1]Delft University of Technology. Water Resources Section. Stevinweg 1, 2628 CN Delft, The Netherlands.
[2]Tecnológico de Costa Rica. Escuela de Ingeniería Forestal. 159-7050, Cartago, Costa Rica.
[3]Independent Researcher

Correspondence: César Dionisio Jiménez–Rodríguez (cdjimenezcr@gmail.com)

Abstract. Forest evaporation exports a vast amount of water vapor from land ecosystems into the atmosphere. Meanwhile, evaporation during rain events is neglected or considered of minor importance in dense ecosystems. Air convection moves the water vapor upwards leading the formation of large invisible vapor plumes, while the identification of visible vapor plumes has not been studied yet. This work describes the formation process of vapor plumes in a tropical wet forest as evidence of evaporation processes happening during rain events. In the dry season of 2018 at La Selva Biological Station (LSBS) in Costa Rica it was possible to spot visible vapor plumes within the forest canopy. The combination of time–lapse videos at the canopy top with meteorological measurements along the canopy profile allowed to identify the conditions required for this process to happen. This phenomenon happened only during rain events, where evaporation measurements showed contributions of 1.8 mm d^{-1}. Visible vapor plumes during day time occurred on the presence of precipitation (P), air convection identified by the temperature gradient ($\frac{\Delta\Theta_v}{\Delta z}$) at 2 m height, and a lifting condensation level at 43 m height ($Z_{lcl.43}$) smaller than 100 m.

1 Introduction

Forest cover in tropical regions is endangered by deforestation (Curtis et al., 2018; Rosa et al., 2016), compromising the evaporation flux from land. Forest evaporation is a mixture of water vapor originated from water intercepted on plant surfaces, soil water and plant transpiration (Roberts, 1999; Savenije, 2004; Shuttleworth, 1993). Forest evaporation is considered of major importance as a regional and local cooling system (Ellison et al., 2017) as a result of their capacity to recycle the atmospheric moisture at different time scales (van der Ent and Savenije, 2011). The water vapor originated from evaporation at the surface is horizontally transported in the atmosphere by advection (Lavers et al., 2015; Strong et al., 2007), whilst vertical transport is linked to wind shear (Chen et al., 2015) and convection (Trzeciak et al., 2017). Large ecosystems influence the formation of convective clouds at the top of the atmospheric boundary layer (Fuentes et al., 2016; Manoli et al., 2016). This process plays an important role in the formation of precipitation in tropical basins (Adams et al., 2011; van der Ent and Savenije, 2011), because of the contribution of water vapor originated from local evaporation (Brubaker et al., 1993).

https://doi.org/10.5194/hess-2020-14
Preprint. Discussion started: 23 January 2020


Hydrology and Earth System Sciences
Discussions

Evaporation is usually neglected or considered of minor importance during rain events in dense forest ecosystems (Klaassen et al., 1998). This because during rainfall the vapor pressure deficit is close to zero (Bosveld and Bouten, 2003; Loescher et al., 2005; Mallick et al., 2016), reducing the atmospheric water demand and stopping the transpiration process (Gotsch et al., 2014). However, the increment of evaporation with the size of rain events suggest that evaporation also occurs during the events and not only afterwards (Allen et al., 2020). This has been evidenced by discrepancies found between modelled and measured evaporation rates in tropical forests (Schellekens et al., 2000). When it rains part of the precipitation is intercepted and evaporated directly to the atmosphere (David et al., 2006), even when vapor pressure deficit and available radiation are low (Lankreijer et al., 1999). Under high humidity conditions a portion of the precipitation can evaporate after a raindrop splashes on the canopy or the forest floor. This process is known as "splash droplet evaporation" (Dunin et al., 1988; Dunkerley, 2009; Murakami, 2006) and is based on the principle that raindrop size increases with rain intensity. Consequently, when larger drops hit the surface (e.g, ground, leaves, branches) allow the formation of smaller rain droplets that can be easily evaporated after the splash. This process has been pointed out as the main source of evaporation to explain the difference between intercepted water and measured evaporation in studies carried out in banana plants (Bassette and Bussière, 2008) and Eucalyptus plantations (Dunin et al., 1988).

Forest evaporation produce coherent structures of water vapor called plumes, cells or rolls (Couvreux et al., 2010). Plumes of water vapor have been identified above forest ecosystems during day time with high resolution scanning Raman LIDAR technique (Cooper et al., 2006; Kao et al., 2000). These plumes reached heights above the canopy up to 100 m, depicting their importance as water vapor providers at local scale. This phenomenon has been studied in astrophysics (Berg et al., 2016; Sparks et al., 2019), vulcanology (Kern et al., 2017; Sioris et al., 2016), regional and global meteorology (Herman et al., 2017; Knoche and Kunstmann, 2013; Wang, 2003; Wright et al., 2017). However, to the authors best knowledge little attention has been drawn to small events observed during rain events. Additionally, Couvreux et al. (2010) highlighted the lack of sampling techniques able to characterize the occurrence of these plumes close to the surface. This work aims to identify the presence of visible vapor plumes in a Tropical Wet Forest. It also tries to explain when and why these plumes occur using meteorological data vertically distributed along the forest canopy layer.

2 Methodology

2.1 Study Site

The monitoring was carried out at La Selva Biological Station (LSBS) on the Caribbean lowlands of Costa Rica (N: $10°26'0''$ – W: $83°59'0''$). This station registered a mean annual precipitation of 4351 mm yr^{-1}, a mean annual temperature of 26.3 °C, and a mean daily temperature difference of 9.5 °C. A short dry season is present in LSBS between February and April every year, and it is characterized by a reduction in the precipitation without vegetation experiencing a soil water deficit (Sanford Jr. et al., 1994; Lieberman and Lieberman, 1987; Loescher et al., 2005). LSBS is covered by a matrix of old growth and secondary

https://doi.org/10.5194/hess-2020-14
Preprint. Discussion started: 23 January 2020

Hydrology and Earth System Sciences
Discussions

forests, small forest plantations, and permanent plots with mixed tree species (Figure 1). All the instrumentation was placed at the Major Research Infrastructure plot (MRI–plot) of 1.0 ha, located within an old growth forest on the upper terrace of the Puerto Viejo river (Sanford Jr. et al., 1994). The MRI–plot is situated in the upper section of a small hill facing South–West towards an affluent of the Puerto Viejo river. The soil is classified as Andic Humidotropept with a clay and organic matter content of 35 % and 23 %, respectively (Sollins et al., 1994). Tree density in 2017 was 371 trees ha^{-1} of individuals with a tree diameter bigger than 10 cm. The palm *Welfia regia* and the tree *Pentaclethra macroloba* are the most abundant species with 56 trees ha^{-1} and 43 trees ha^{-1}, respectively. Average leaf area index (LAI) in 2005 was 3.56 m^2 m^{-2} (Tang et al., 2012). The plot is located within a stable forest plot in terms of changes in canopy height and tree biomass fixation (Dubayah et al., 2010).

2.2 Experimental Design

The monitoring was carried out on the MRI–plot in the highest tower (43 m), which is located within a depression of the forest canopy (Figure 1). Along the vertical axis of the tower, the air temperature (°C) and relative humidity (%) were measured with HOBO® smart sensors (part code: S-THB-M008). The sensors were located at 2 m, 8 m and 43 m height, placed at a distance of 1.5 m from the tower and protected with a radiation shield (HOBO® part code: RS-3) of 10 cm diameter. At the highest point of the tower, the precipitation (mm min^{-1}) was recorded with a Davis® rain gauge. Soil temperature (°C) was measured in two different locations at 5 cm and 15 cm depth with a soil temperature sensor (HOBO® part code: TMC20-HD). Soil moisture (Θ, m^3 m^{-3}) was measured at the same locations as soil temperature at 5 cm depth with an ECH_2O® EC sensor. Soil temperature was recorded with a 4-channel data logger (HOBO® part code: U12-008) and the other sensors with a USB Micro Station (HOBO® part code: H21-USB) every 5 min. A Bushnell® Natureview® Essential HD camera (12 megapixels) was installed at the top of the tower facing North–West.

2.3 Monitoring Period

All environmental variables were monitored between 2018-01-24 and 2018-03-26 (see Appendix A). The camera was installed to collect photographs above the canopy between 2018-03-21 and 2018-03-25 at different time windows (see Appendix B). The photographs were collected continuously from 5:00 to 18:30 hours local time (UTC-6). These pictures were used to determine the timing when the vapor plumes were visible at the MRI–plot. The photographs were classified into three conditions (Figure 2):

- Clear View: includes all the pictures with clear and cloudy sky where the canopy is clearly visible and there is neither mist nor plumes present (Figure 2 A and B).
- Mist and Fog: includes the presence of a homogeneous blurry view of the canopy. The blurriness of each picture varies depending on the humidity conditions. Special care was taken to prevent the erroneous classification of photographs affected by a fogged–up lens. This category is called "mist" from now onwards (Figure 2 C).

https://doi.org/10.5194/hess-2020-14
Preprint. Discussion started: 23 January 2020

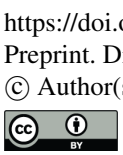

Hydrology and Earth System Sciences
Discussions
Open Access
EGU

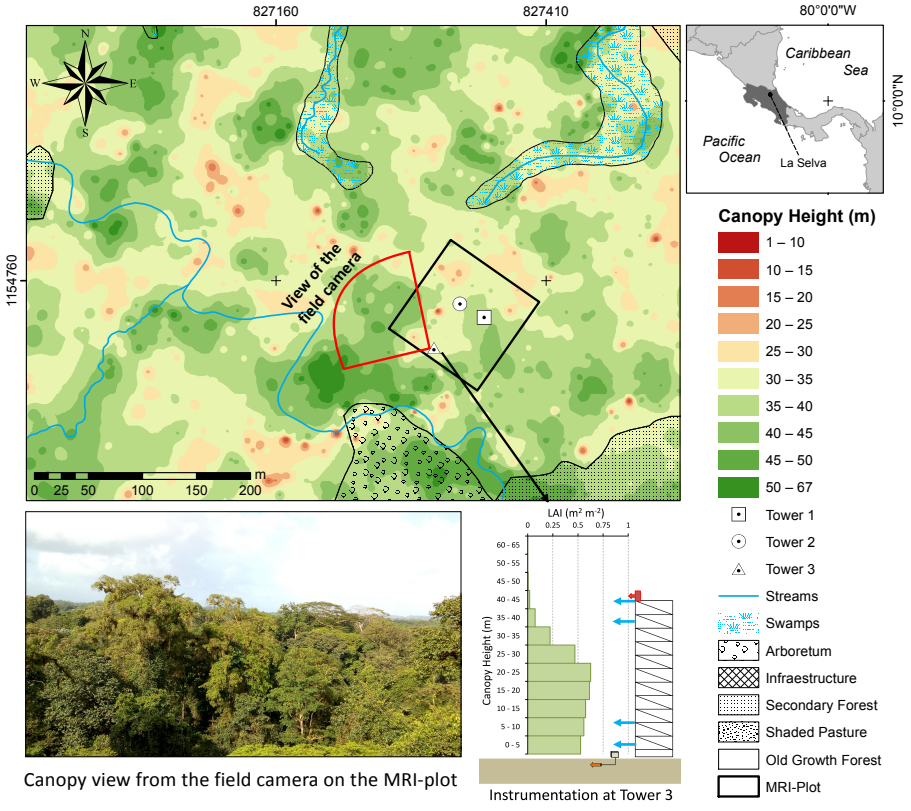

Figure 1. Canopy height of the area surrounding the Major Research Infrastructure plot (MRI–plot) at La Selva Biological Station, Costa Rica. The photograph in the map shows a view from the field camera at the top of the tower (red box with arrow). The blue arrows along the Tower 3 diagram show the locations of temperature and relative humidity sensors.

– Plumes: includes the presence of buoyant vapor clouds risen from the forest canopy (Figure 2 D). These cloud bodies change their vertical position in consecutive frames. Rising vapor plumes can be observed in the online video of 2018-03-24 available at https://doi.org/10.4121/uuid:997cc9d8-2281-453e-b631-5f93cfebe00e (Jiménez-Rodríguez et al., 2019c).

2.4 Data Analysis

Data processing and analysis was performed with the open source software R (R Core Team, 2017). All temperatures were converted from K to °C. Superficial soil temperature ($T_{s.0}$, °C) was estimated with equation 1 (Holmes et al., 2008). This equation describes the diurnal variations of soil temperature as sine waves depending on the 24 h moving averages of soil temperature at 5 cm depth ($T_{s.5}$, °C). The daily amplitude of air temperature (T_A, °C) is defined as the difference between $T_{s.5}$ and the air temperature at 2 m (T_{2m}). The oscillations are determined by the damping depth (ν, m) which is calculated with equation 2. Depth difference between the T_{ss} and $T_{s.5}$ is defined as z_b (m). The sine pattern depends on the angular frequency

https://doi.org/10.5194/hess-2020-14
Preprint. Discussion started: 23 January 2020

Hydrology and Earth System Sciences
Discussions
Open Access
EGU

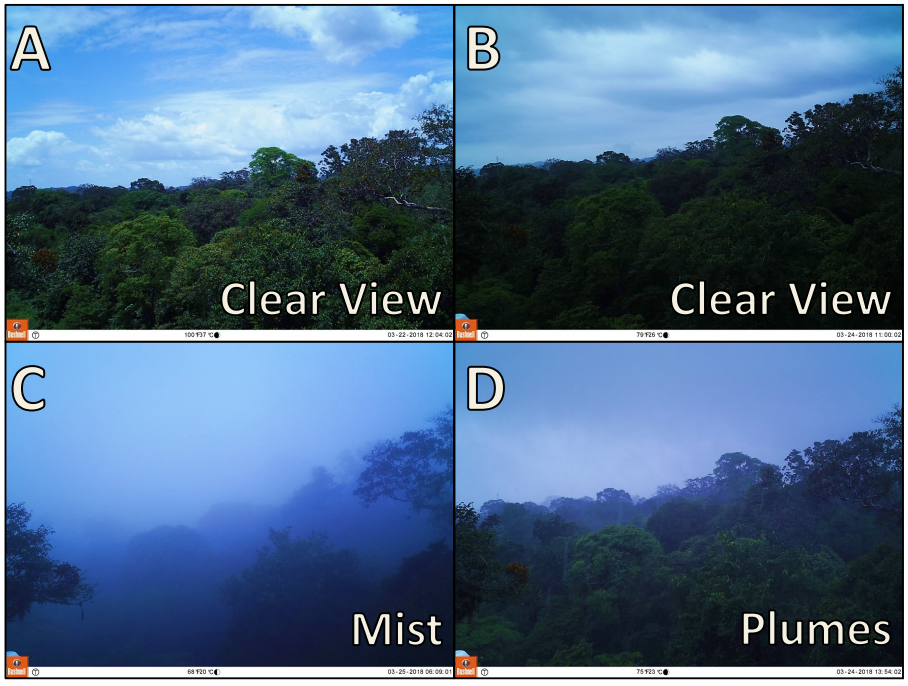

Figure 2. Visual monitoring showing the 3 conditions used to classify the canopy photographs on the time-lapse videos. The pictures A and B show the "Clear View" classification, picture A on a sunny day and picture B during rain. Picture C describes the Mist and picture D shows the plumes rising from the forest canopy.

(ω, s^{-1}), time (t) in s and ϕ (-) as a constant for phase change. Equation 3 is used to determine ω with τ (s) as the wave period. Equation 2 calculates ν with the soil thermal diffusivity (η, $m^2\,s^{-1}$) and ω. Equation 4 (Nakshabandi and Kohnke, 1965) is used to determine η, where ρ_s is the soil bulk density of 0.76 g cm^{-3} (Sollins et al., 1994) for the experimental plot, c_s is the specific heat for clay soils (837.36 W kg^{-1} °C^{-1}) and k is the soil thermal conductivity of 1.58 W m^{-1} °C^{-1} (Pielke, 2013). These last two parameters were chosen according to the soil water conditions during the monitoring period, which was close to soil field capacity (see Appendix A).

$$T_{s.0} = T_{s.5} + T_A\, e^{\left(\frac{-z_s}{\nu}\right)} \sin\left(\omega t - \frac{z_b}{\nu} + \phi\right) \tag{1}$$

$$\nu = \sqrt{\frac{2\eta}{\omega}} \tag{2}$$

$$\omega = \frac{2\pi}{\tau} \tag{3}$$

https://doi.org/10.5194/hess-2020-14
Preprint. Discussion started: 23 January 2020


Hydrology and Earth System Sciences
Discussions

$$\eta = \frac{k}{\rho_s c_s} \tag{4}$$

Virtual potential temperature (θ_v, °) of the air was calculated to take into account the variation in the adiabatic lapse rate due to changes in pressure (Barr et al., 1994; Stull, 1988, 2016). For saturated (cloudy) air conditions equation 5 calculates the θ_v based on the water-vapor mixing ratio (ψ_s) of the moist air, the liquid water mixing ratio (ψ_L) and the virtual temperature (θ). The parameters ψ_s and ψ_L were determined using the vapor pressure deficit of the air on each height (Stull, 2016). The virtual temperature was estimated with equation 6 where Γ_d is the dry adiabatic lapse rate near the surface (0.0098 °C m^{-1}), z is the height above the ground in m and T_z is the air temperature at the same heights.

$$\theta_{v.z} = \theta_z(1 + 0.608\,\psi_s - \psi_L) \tag{5}$$

$$\theta_z = T_z + \Gamma_d\, z \tag{6}$$

Convection can be identified by evaluating the temperature gradient ($\frac{\Delta\theta_v}{\Delta z}$). Values of $\frac{\Delta\theta_v}{\Delta z} > 0$ are linked to stable stratification, meanwhile $\frac{\Delta\theta_v}{\Delta z} < 0$ show an unstable stratification, which will drive convection.

The condensation of vapor close to the forest canopy can be identified by calculating the lifting condensation level (z_{lcl}) in m with equation 7. This equation determines the elevation at which a parcel of air condensates allowing the formation of clouds. This equation uses the difference between air temperature (T_z) and dew point temperature ($T_{dew.z}$) at one specific height (z), divided by the difference between Γ_d and the moist adiabatic lapse rate (Γ_{dew}) at T_z and $T_{dew.z}$ (Stull, 2016).

$$z_{lcl} = \frac{T_z - T_{dew.z}}{\Gamma_d - \Gamma_{dew}} \tag{7}$$

The energy balance equation (Equation 8) was used to estimate the evaporation (E_z) in m s^{-1} at 2 m, 8 m and 43 m height. In this equation, G is the ground heat flux (W m^{-2}), $R_{n.z}$ is the net radiation (W m^{-2}), H_z the sensible heat flux (W m^{-2}), ρ_w is the water density (1000 kg m^{-3}) and λ the latent heat of vaporization (2.405×10^6 J kg^{-1}). $R_{n.z}$ and H_z are estimated at 2 m, 8 m and 43 m. The estimation of all the fluxes is described in detail by Jiménez-Rodríguez et al. (2019a). Equation 8 is based on the vertical transport of heat and neglects the advected energy on the forest canopy as a consequence of the lack of more detailed measurements (e.g, eddy covariance system).

$$E_z = \frac{R_{n.z} - H_z - G}{\rho_w \lambda} \tag{8}$$

https://doi.org/10.5194/hess-2020-14
Preprint. Discussion started: 23 January 2020

Hydrology and Earth System Sciences
Discussions

3 Results and Discussion

The monitoring period experienced a diurnal variation in air temperature along the vertical profile of the canopy, with a temperature difference of more than 10 °C at 43 m and less than 7 °C at 2 m height (Figure 3). The highest temperatures were registered at 43 m height reaching more than 30 °C, decreasing in magnitude towards the forest floor. These peak temperatures were recorded around noon with differences up to 5 °C between the air temperature at 43 m and 2 m height. The $T_{s.0}$ oscillates between 20.7 °C and 25.4 °C. The amplitude of the oscillation increased with the sunniest days but the daily difference does not exceed the 4 °C. The maximum Θ value was 0.47 m^3 m^{-3} during the heavy rains, almost reaching the saturation point for clay soils of 0.50 m^3 m^{-3} (Saxton and Rawls, 2006). The minimum Θ was recorded after the driest period just before the rains on 2018-03-24 (0.42 m^3 m^{-3}) getting close to soil field capacity for clay soils (Saxton and Rawls, 2006). Evaporation always occurs during daytime on all sampling days (Figure 3). During the four sunny days the evaporation was larger than 5 mm d^{-1}, with a contribution of more than 1.0 mm d^{-1} from 8 m height and no more than 0.7 mm d^{-1} from 2 m height. In contrast, during 2018-03-24 the continuous rains sum up 58.7 mm d^{-1} and the evaporation was estimated as 1.8 mm d^{-1} at 43 m and only 0.2 d^{-1} at 2 m height (Table 1).

Table 1. Summary of daily precipitation and evaporation at 43 m, 8 m and 2 m height estimated based on the meteorological data collected on site.

Date	Precipitation	Evaporation (mm d^{-1})		
	(mm d^{-1})	0–43 m	0–8 m	0–2 m
2018-03-21	0.0	6.0	1.5	0.7
2018-03-22	0.0	5.4	1.1	0.4
2018-03-23	4.6	5.8	1.1	0.3
2018-03-24	58.7	1.8	0.5	0.2
2018-03-25	0.0	5.3	1.2	0.5

Note: all evaporation values corresponds to the water vapor produced from the forest floor up to the specified height.

During the visual monitoring with the field camera, clear view conditions were predominant along four days (Figure 3). These days were characterized by sunny conditions with temperatures above the 25 °C, no large rain events and a decreasing trend in soil moisture. Also, on 2018-03-24 it was possible to identify three short periods with clear view conditions in between the rains. Mist formation was identify on 2018-03-23 and 2018-03-25 before 7:00 a.m. Meanwhile the photographs of the other sampling days did not show mist formation because of its timing. These mist events were linked with superficial soil temperatures higher than 2 °C respect to air temperature. Finally, the vapor plumes were visible only during rainy conditions on 2018-03-24 (videos available at Jiménez-Rodríguez et al. (2019c)). Soil temperatures during this day were warmer than the

https://doi.org/10.5194/hess-2020-14
Preprint. Discussion started: 23 January 2020


Hydrology and Earth System Sciences
Discussions

air column along the forest canopy (Figure 3).

Evaporation during sunny days provided the conditions to form vapor plumes as those ones described by Cooper et al. (2006) and Kao et al. (2000). The evaporation peaks during these days occurred around noon, registering a z_{lcl} higher than 500 m (Figure 3) which is the height required to form clouds and be visible. This is the reason why is not possible to see the vapor rising from the surface. The vapor plumes were visible on the day with continuous precipitation (2018-03-24). On this day, the Z_{lcl} dropped beneath 100 m because during rain events the θ_{v} of all the air column dropped quickly. This drop kept the θ_{v} beneath the superficial soil temperature, allowing a localized convection event. This convection process forced the evaporated water to move upwards forming buoyant clouds close to the forest surface. The evaporation during rain events is the result of the splash droplet evaporation process (Murakami, 2006; Dunkerley, 2009), which can provide water vapor as a consequence of the fragmentation of raindrops when hitting the surface.

Energy convection plays an important role in forest ecosystems during night time (Bosveld et al., 1999). This is a consequence of the mass transport capacity of the intermittent nocturnal convective fluxes (Cooper et al., 2006). The convection process is forced by the ground heat flux (Jacobs et al., 1994), which is enhanced by the larger soil moisture in the clay soil which increases the soil heat capacity (Abu-Hamdeh, 2003). A coupled canopy system enables sensible heat and water vapor transport from the soil to the atmosphere just above the canopy layer (Göckede et al., 2007). This facilitates the generation of the convection process, allowing the ascending warm air to cool down at the canopy top and condensate forming the visible water vapor plumes. The condensation releases heat (Goosse, 2015), driving the convection. Vapor plumes are always present as a consequence of the moisture exchange between the surface and the atmosphere (Lawford, 1996), where evaporation from land covers with enough water supply provides the required air moisture (Kao et al., 2000). However, the conditions needed to form a visible buoyant cloud close to the surface require a big difference in air temperature over height. Temperature gradient at 43 m, 8 m and 2 m is negative during plumes and mist conditions, meanwhile clear view conditions has a larger range with more positive values (see Appendix C).

Visible vapor plumes are the result of the condensation of water vapor rising from a warmer surface. When a column of warm humid air reaches a lower density than air above, the water vapor condensates around aerosols in the air allowing the formation of clouds (Stull, 2016). In this regard, there are two sources of aerosols at LSBS. One source is linked to windy carrying aerosols from nearby agricultural land uses (Loescher et al., 2004). The second source is linked to convective rains that characterize the dry season at LSBS. These rains transport from the free troposphere into the boundary layer the required aerosols for the condensation process and later formation of clouds (Wang et al., 2016). Meanwhile the "splash droplet evaporation" process (Murakami, 2006) provides the main source of water vapor after rain drops hit the canopy and soil surfaces.

Cloud formation usually happens high above the surface boundary layer where the forest canopy is located, but available information of cloud formation close to the forest canopy is scarce. The temperature gradient ($\frac{\Delta\theta_{\mathrm{v}}}{\Delta z}$) at 43 m, 8 m and 2 m is

https://doi.org/10.5194/hess-2020-14
Preprint. Discussion started: 23 January 2020

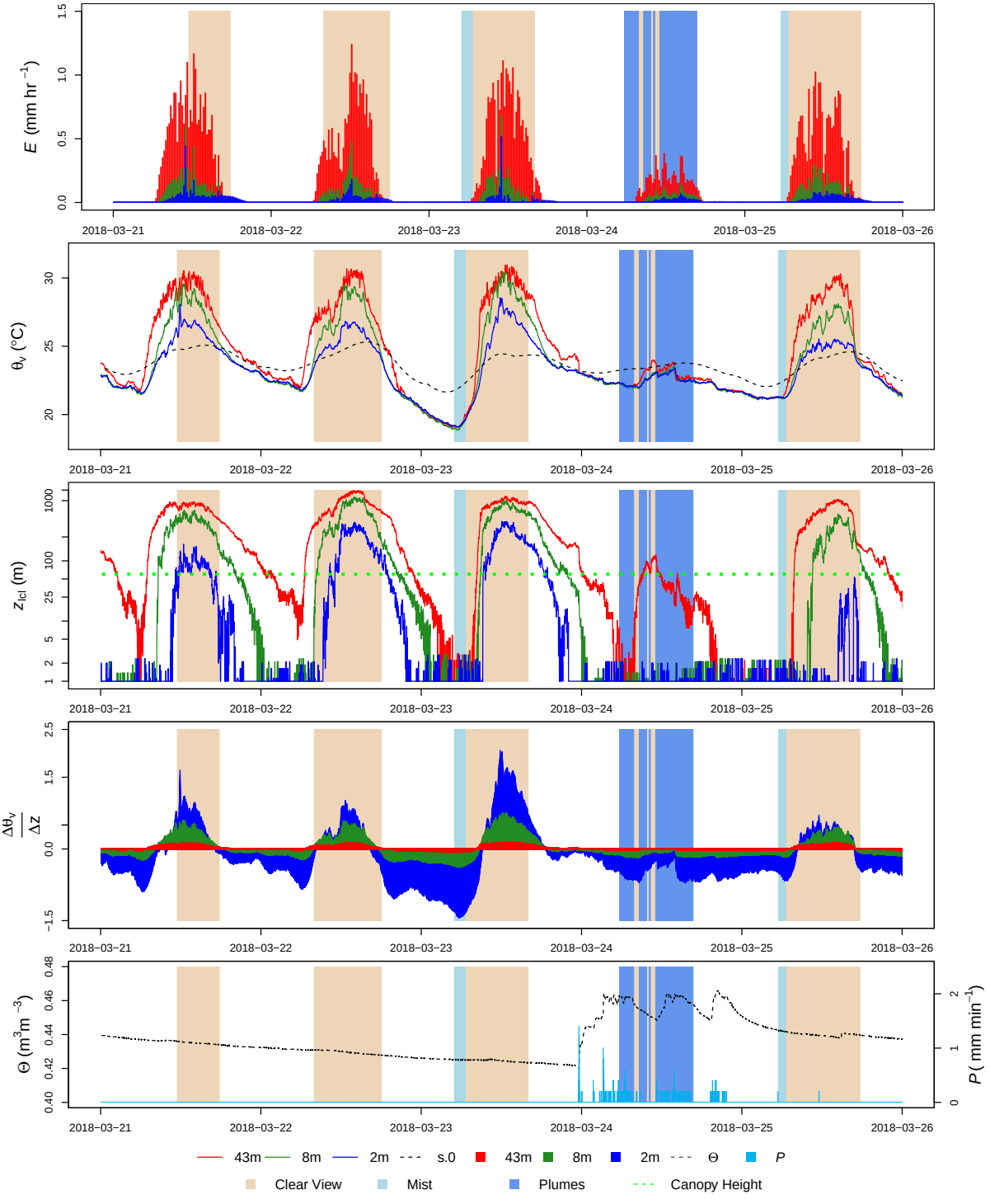

Figure 3. Evaporation (E), Virtual potential temperature (θ_v), lifting condensation level (z_{lcl}) in an untransformed semi–logarithmic scale and temperature gradient ($\frac{\Delta\theta_v}{\Delta z}$) at 43 m, 8 m and 2 m height. Additionally, precipitation (P) and soil moisture (Θ) are also shown during the visual monitoring between 2018-03-21 and 2018-03-25. Background colored areas denoted the three categories in which the photographs were classified: Clear View, Mist and Plumes.

https://doi.org/10.5194/hess-2020-14
Preprint. Discussion started: 23 January 2020

Hydrology and Earth System Sciences
Discussions

negative during plumes and mist conditions, meanwhile clear view conditions have a larger range with more positive gradients. Lifting condensation level is a key element that allowed to differentiate between plumes and mist conditions (see Appendix C). The combination of variables such as Z_{lcl}, $\frac{\Delta\theta_{\mathrm{v}}}{\Delta z}$, and P allows to identify the formation of vapor plumes in Tropical Wet Forests (Figure 4). The z_{lcl} is the height in the atmosphere at which a parcel of moist air becomes saturated if experience a forced ascent (Stull, 2016). It provides an estimate of the height at which the clouds can be formed. The temperature gradient is an indicator of how easily a parcel of air can be lifted (Spellman, 2012) and can be used as a proxy of the atmospheric stability. During unstable atmospheric conditions ($\frac{\Delta\theta_{\mathrm{v}}}{\Delta z} < 0$) is more easy to move upwards the parcels of air than under stable conditions ($\frac{\Delta\theta_{\mathrm{v}}}{\Delta z} > 0$). Finally, precipitation saturates the air column and provides the water vapor after the splash droplet evaporation process on the canopy and forest floor surfaces.

During the full monitoring period at La Selva Biological Station, only 1.4 % of our study period accomplished the conditions required for the formation of visible vapor plumes (precipitation, $Z_{\mathrm{lcl}} < 100\,\mathrm{m}$ and $0 > \frac{\Delta\theta_{\mathrm{v}}}{\Delta z} > -1$). These conditions differ from those needed to form mist. In a tropical wet forest in Costa Rica, fog and mist formation happens before sunrise (Allen et al., 1972). However, fog does not involve the upward convective flux needed for vapor plumes, while mist is affected by this upward convective flux but without rain (Stull, 2016). Vapor plumes are buoyant cloud formations with an identifiable shape Spellman (2012), main characteristics that allow the differentiation from fog and mist events. While mist and fog are formed by microscopic water droplets floating in the air which can reduce the visibility to less than one kilometer in the case of fog or a lesser extent with the mist Spellman (2012).

https://doi.org/10.5194/hess-2020-14
Preprint. Discussion started: 23 January 2020

Hydrology and Earth System Sciences
Discussions

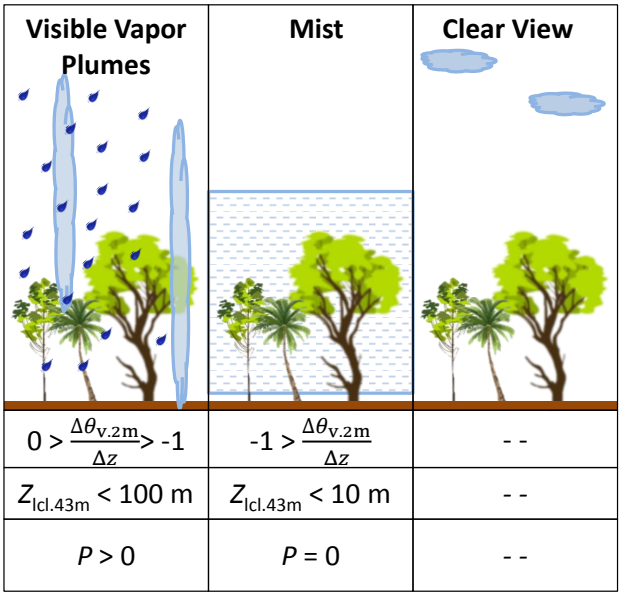

Figure 4. Simplification diagram describing the required conditions to form visible vapor plumes in a Tropical Wet Forest and the differences between mist and clear view conditions.

4 Conclusions

The visual monitoring captured the formation of visible vapor plumes close to the surface boundary layer of a Tropical Wet Forest (TWF) during rainy conditions. These visible plumes are the visual evidence of evaporation processes happening during rain events, where the splash droplet evaporation process provides the required water vapor to form visible vapor plumes. This water vapor is part of the intercepted water evaporated from the forest floor and plant surfaces since transpiration is likely reduced by the low vapor pressure deficit. It is raised up by air convection driven by warm soil temperatures. Finally, condensing close to the forest canopy due to the drop in the virtual potential air temperature along the forest air column. Consequently, this phenomenon can be identified in TWF when precipitation occurs, the lifting condensation level at 43 m height (Z_{lcl}) is lower than 100 m, and the temperature gradient ($\frac{\Delta\theta_{\mathrm{v}}}{\Delta z}$) at 2 m height is between 0 and -1 °C m^{-1}. Contrary to the vapor plumes, mist appear when no precipitation occurs ($P = 0$), Z_{lcl} at 43 m is less than 10 m and $\frac{\Delta\theta_{\mathrm{v}}}{\Delta z}$ is less than -0.5 °C m^{-1}. This work also brings the attention to the forest evaporation role during rain events, where little information is still available.

Competing interests. The authors declare that they have no conflict of interest.

https://doi.org/10.5194/hess-2020-14
Preprint. Discussion started: 23 January 2020

Hydrology and Earth System Sciences
Discussions
Open Access
EGU

Acknowledgements. This work was carried out with a fellowship from the Organization for Tropical Studies (Glaxo Centroamerica Fellowship–Fund 502). With the aid of a scholarship from PINN-MICITT Costa Rica (contract: PED-032-2015-1) and the aid of the grant 863.15.022 from The Netherlands Organization for Scientific Research (NWO). Also, NASA's funding NNX12AN43H and 80NSSC18K0708 for providing the LAI data sets. Special thanks to Bernal Matarrita, Orlando Vargas, Wagner López, Danilo Brenes, Diego Dierick, Enrique Castro and Marisol Luna for their help and advice in the research station. Finally, to all the staff of the OTS for its willingness to support our project.

Data availability. Time lapse videos are available online in the 4TU data repository at https://data.4tu.nl/repository/uuid:997cc9d8-2281-453e-b631-5f93cfebe00e (Jiménez-Rodríguez et al., 2019c). Meteorological data used in this manuscript are available online in the 4TU data repository (https://doi.org/10.4121/uuid:e70993d2-5852-4f63-9aff-39451fbd3fde; Jiménez-Rodríguez et al. (2019b).

https://doi.org/10.5194/hess-2020-14
Preprint. Discussion started: 23 January 2020

References

Abu-Hamdeh, N. H.: Thermal Properties of Soils as affected by Density and Water Content, Biosystems Engineering, 86, 97–102, https://doi.org/10.1016/S1537-5110(03)00112-0, 2003.

Adams, D. K., Fernandes, R. M. S., Kursinski, E. R., Maia, J. M., Sapucci, L. F., Machado, L. A. T., Vitorello, I., Monico, J. F. G., Holub, K. L., Gutman, S. I., Filizola, N., and Bennett, R. A.: A dense GNSS meteorological network for observing deep convection in the Amazon, Atmospheric Science Letters, 12, 207–212, https://doi.org/10.1002/asl.312, 2011.

Allen, L. H., Lemon, E., and Müller, L.: Environment of a Costa Rican Forest, Ecology, 53, 102–111, https://doi.org/10.2307/1935714, 1972.

Allen, S. T., Aubrey, D. P., Bader, M. Y., Coenders-Gerrits, M., Friesen, J., Gutmann, E. D., Guillemette, F., Jiménez-Rodríguez, C., Keim, R. F., Klamerus-Iwan, A., Mendieta-Leiva, G., Porada, P., Qualls, R. G., Schilperoort, B., Stubbins, A., and Van Stan II, J. T.: Key Questions on the Evaporation and Transport of Intercepted Precipitation, pp. 269–280, Springer International Publishing, Cham, https://doi.org/10.1007/978-3-030-29702-2_16, 2020.

Barr, A. G., King, K. M., Gillespie, T. J., Den Hartog, G., and Neumann, H. H.: A comparison of bowen ratio and eddy correlation sensible and latent heat flux measurements above deciduous forest, Boundary-Layer Meteorology, 71, 21–41, https://doi.org/10.1007/BF00709218, 1994.

Bassette, C. and Bussière, F.: Partitioning of splash and storage during raindrop impacts on banana leaves, Agricultural and Forest Meteorology, 148, 991 – 1004, https://doi.org/10.1016/j.agrformet.2008.01.016, 2008.

Berg, J., Goldstein, D., Varghese, P., and Trafton, L.: DSMC simulation of Europa water vapor plumes, Icarus, 277, 370–380, https://doi.org/10.1016/j.icarus.2016.05.030, 2016.

Bosveld, F. C. and Bouten, W.: Evaluating a Model of Evaporation and Transpiration with Observations in a Partially Wet Douglas-Fir Forest, Boundary-Layer Meteorology, 108, 365–396, https://doi.org/10.1023/A:1024148707239, 2003.

Bosveld, F. C., Holtslag, A. M., and Van Den Hurk, B. J.: Nighttime convection in the interior of a dense Douglas fir forest, Boundary-Layer Meteorology, 93, 171–195, https://doi.org/10.1023/A:1002039610790, 1999.

Brubaker, K. L., Entekhabi, D., and Eagleson, P. S.: Estimation of Continental Precipitation Recycling, Journal of Climate, 6, 1077–1089, https://doi.org/10.1175/1520-0442(1993)006<1077:EOCPR>2.0.CO;2, 1993.

Chen, Q., Fan, J., Hagos, S., Gustafson Jr., W. I., and Berg, L. K.: Roles of wind shear at different vertical levels: Cloud system organization and properties, Journal of Geophysical Research: Atmospheres, 120, 6551–6574, https://doi.org/10.1002/2015JD023253, 2015.

Cooper, D., Leclerc, M., Archuleta, J., Coulter, R., Eichinger, W., Kao, C., and Nappo, C.: Mass exchange in the stable boundary layer by coherent structures, Agricultural and Forest Meteorology, 136, 114–131, https://doi.org/10.1016/j.agrformet.2004.12.012, advances in Surface-Atmosphere Exchange - A Tribute to Marv Wesely, 2006.

Couvreux, F., Hourdin, F., and Rio, C.: Resolved Versus Parametrized Boundary-Layer Plumes. Part I: A Parametrization-Oriented Conditional Sampling in Large-Eddy Simulations, Boundary-Layer Meteorology, 134, 441–458, https://doi.org/10.1007/s10546-009-9456-5, 2010.

Curtis, P. G., Slay, C. M., Harris, N. L., Tyukavina, A., and Hansen, M. C.: Classifying drivers of global forest loss, Science, 361, 1108–1111, https://doi.org/10.1126/science.aau3445, 2018.

David, J. S., Valente, F., and Gash, J. H.: Evaporation of Intercepted Rainfall, in: Encyclopedia of Hydrological Sciences, chap. 43, American Cancer Society, https://doi.org/10.1002/0470848944.hsa046, 2006.

https://doi.org/10.5194/hess-2020-14
Preprint. Discussion started: 23 January 2020

Dubayah, R. O., Sheldon, S. L., Clark, D. B., Hofton, M. A., Blair, J. B., Hurtt, G. C., and Chazdon, R. L.: Estimation of tropical forest height and biomass dynamics using lidar remote sensing at La Selva, Costa Rica, Journal of Geophysical Research: Biogeosciences, 115, https://doi.org/10.1029/2009JG000933, 2010.

Dunin, F. X., O'Loughlin, E. M., and Reyenga, W.: Interception loss from eucalypt forest: Lysimeter determination of hourly rates for long term evaluation, Hydrological Processes, 2, 315–329, https://doi.org/10.1002/hyp.3360020403, 1988.

Dunkerley, D. L.: Evaporation of impact water droplets in interception processes: Historical precedence of the hypothesis and a brief literature overview, Journal of Hydrology, 376, 599 – 604, https://doi.org/10.1016/j.jhydrol.2009.08.004, 2009.

Ellison, D., Morris, C. E., Locatelli, B., Sheil, D., Cohen, J., Murdiyarso, D., Gutierrez, V., van Noordwijk, M., Creed, I. F., Pokorny, J., Gaveau, D., Spracklen, D. V., Tobella, A. B., Ilstedt, U., Teuling, A. J., Gebrehiwot, S. G., Sands, D. C., Muys, B., Verbist, B., Springgay, E., Sugandi, Y., and Sullivan, C. A.: Trees, forests and water: Cool insights for a hot world, Global Environmental Change, 43, 51–61, https://doi.org/10.1016/j.gloenvcha.2017.01.002, 2017.

Fuentes, J. D., Chamecki, M., Nascimento dos Santos, R. M., Von Randow, C., Stoy, P. C., Katul, G., Fitzjarrald, D., Manzi, A., Gerken, T., Trowbridge, A., Souza Freire, L., Ruiz-Plancarte, J., Furtunato Maia, J. M., TÃ³ta, J., Dias, N., Fisch, G., Schumacher, C., Acevedo, O., Rezende Mercer, J., and YaÃ±ez-Serrano, A. M.: Linking Meteorology, Turbulence, and Air Chemistry in the Amazon Rain Forest, Bulletin of the American Meteorological Society, 97, 2329–2342, https://doi.org/10.1175/BAMS-D-15-00152.1, 2016.

Göckede, M., Thomas, C., Markkanen, T., Mauder, M., Ruppert, J., and Foken, T.: Sensitivity of Lagrangian Stochastic footprints to turbulence statistics, Tellus B: Chemical and Physical Meteorology, 59, 577–586, https://doi.org/10.1111/j.1600-0889.2007.00275.x, 2007.

Goosse, H.: The energy balance, hydrological and carbon cycles, in: Climate System Dynamics and Modelling, chap. 2, Cambridge University Press, 2015.

Gotsch, S. G., Asbjornsen, H., Holwerda, F., Goldsmith, G. R., Weintraub, A. E., and Dawson, T. E.: Foggy days and dry nights determine crown-level water balance in a seasonal tropical montane cloud forest, Plant, Cell & Environment, 37, 261–272, https://doi.org/10.1111/pce.12151, 2014.

Herman, R. L., Ray, E. A., Rosenlof, K. H., Bedka, K. M., Schwartz, M. J., Read, W. G., Troy, R. F., Chin, K., Christensen, L. E., Fu, D., Stachnik, R. A., Bui, T. P., and Dean-Day, J. M.: Enhanced stratospheric water vapor over the summertime continental United States and the role of overshooting convection, Atmospheric Chemistry and Physics, 17, 6113–6124, https://doi.org/10.5194/acp-17-6113-2017, 2017.

Holmes, T. R. H., Owe, M., De Jeu, R. A. M., and Kooi, H.: Estimating the soil temperature profile from a single depth observation: A simple empirical heatflow solution, Water Resources Research, 44, 1–11, https://doi.org/10.1029/2007WR005994, 2008.

Jacobs, A. F. G., Van Boxel, J. H., and El-Kilani, R. M. M.: Nighttime free convection characteristics within a plant canopy, Boundary-Layer Meteorology, 71, 375–391, https://doi.org/10.1007/BF00712176, 1994.

Jiménez-Rodríguez, C. D., Coenders-Gerrits, M., Wenninger, J., Gonzalez-Angarita, A., and Savenije, H.: Contribution of understory evaporation in a tropical wet forest, Hydrology and Earth System Sciences Discussions, 2019, 1–32, https://doi.org/10.5194/hess-2019-566, https://www.hydrol-earth-syst-sci-discuss.net/hess-2019-566/, 2019a.

Jiménez-Rodríguez, C. D., González-Angarita, A. P., Coenders-Gerrits, A., Savenije, H., and Wenninger, J.: Meteorological data and isotope signatures of water samples collected at La Selva., https://doi.org/10.4121/uuid:e70993d2-5852-4f63-9aff-39451fbd3fde, 2019b.

Jiménez-Rodríguez, C. D., González-Angarita, A. P., and Coenders-Gerrits, A. M. J.: Vapor Plumes Video at La Selva Biological Station. 4TU.Centre for Research Data. Dataset, *4TU.Centre for Research Data* https://data.4tu.nl/repository/uuid:997cc9d8-2281-453e-b631-5f93cfebe00e, 2019c.

https://doi.org/10.5194/hess-2020-14
Preprint. Discussion started: 23 January 2020

Kao, C.-Y., Hang, Y.-H., Cooper, D., Eichinger, W., Smith, W., and Reisner, J.: High-resolution modeling of LIDAR data: Mechanisms governing surface water vapor variability during SALSA, Agricultural and Forest Meteorology, 105, 185 – 194, https://doi.org/10.1016/S0168-1923(00)00182-9, 2000.

Kern, C., Masias, P., Apaza, F., Reath, K. A., and Platt, U.: Remote measurement of high preeruptive water vapor emissions at Sabancaya volcano by passive differential optical absorption spectroscopy, Journal of Geophysical Research: Solid Earth, 122, 3540–3564, https://doi.org/10.1002/2017JB014020, 2017.

Klaassen, W., Bosveld, F., and de Water, E.: Water storage and evaporation as constituents of rainfall interception, Journal of Hydrology, 212–213, 36–50, https://doi.org/10.1016/S0022-1694(98)00200-5, 1998.

Knoche, H. R. and Kunstmann, H.: Tracking atmospheric water pathways by direct evaporation tagging: A case study for West Africa, Journal of Geophysical Research: Atmospheres, 118, 12,345–12,358, https://doi.org/10.1002/2013JD019976, 2013.

Lankreijer, H., Lundberg, A., Grelle, A., Lindroth, A., and Seibert, J.: Evaporation and storage of intercepted rain analysed by comparing two models applied to a boreal forest, Agricultural and Forest Meteorology, 98-99, 595–604, https://doi.org/10.1016/S0168-1923(99)00126-4, http://www.sciencedirect.com/science/article/pii/S0168192399001264, 1999.

Lavers, D. A., Ralph, F. M., Waliser, D. E., Gershunov, A., and Dettinger, M. D.: Climate change intensification of horizontal water vapor transport in CMIP5, Geophysical Research Letters, 42, 5617–5625, https://doi.org/10.1002/2015GL064672, 2015.

Lawford, R.: Some scientific questions and issues for the GEWEX Continental-scale International Project (GCIP) research community, in: Proceedings of the Second International Science Conference on Global Energy and Water Cycle, June 17–21, Washington, DC., pp. 162–167, 1996.

Lieberman, D. and Lieberman, M.: Forest tree growth and dynamics at La Selva, Costa Rica (1969-1982), Journal of Tropical Ecology, 3, 347–358, https://doi.org/10.1017/S0266467400002327, 1987.

Loescher, H., Gholz, H., Jacobs, J., and Oberbauer, S.: Energy dynamics and modeled evapotranspiration from a wet tropical forest in Costa Rica, Journal of Hydrology, 315, 274–294, https://doi.org/10.1016/j.jhydrol.2005.03.040, 2005.

Loescher, H. W., Bentz, J. A., Oberbauer, S. F., Ghosh, T. K., Tompson, R. V., and Loyalka, S. K.: Characterization and dry deposition of carbonaceous aerosols in a wet tropical forest canopy, Journal of Geophysical Research: Atmospheres, 109, https://doi.org/10.1029/2002JD003353, 2004.

Mallick, K., Trebs, I., Boegh, E., Giustarini, L., Schlerf, M., Drewry, D. T., Hoffmann, L., von Randow, C., Kruijt, B., Araùjo, A., Saleska, S., Ehleringer, J. R., Domingues, T. F., Ometto, J. P. H. B., Nobre, A. D., de Moraes, O. L. L., Hayek, M., Munger, J. W., and Wofsy, S. C.: Canopy-scale biophysical controls of transpiration and evaporation in the Amazon Basin, Hydrology and Earth System Sciences, 20, 4237–4264, https://doi.org/10.5194/hess-20-4237-2016, 2016.

Manoli, G., Domec, J.-C., Novick, K., Oishi, A. C., Noormets, A., Marani, M., and Katul, G.: Soilâ€“plantâ€“atmosphere conditions regulating convective cloud formation above southeastern US pine plantations, Global Change Biology, 22, 2238–2254, https://doi.org/10.1111/gcb.13221, 2016.

Murakami, S.: A proposal for a new forest canopy interception mechanism: Splash droplet evaporation, Journal of Hydrology, 319, 72 – 82, https://doi.org/10.1016/j.jhydrol.2005.07.002, 2006.

Nakshabandi, G. A. and Kohnke, H.: Thermal conductivity and diffusivity of soils as related to moisture tension and other physical properties, Agricultural Meteorology, 2, 271–279, https://doi.org/10.1016/0002-1571(65)90013-0, 1965.

Pielke, R.: Mesoscale Meteorological Modeling, International Geophysics, Elsevier Science, https://books.google.nl/books?id=ExlFulltapcC, 2013.

https://doi.org/10.5194/hess-2020-14
Preprint. Discussion started: 23 January 2020

R Core Team: R: A Language and Environment for Statistical Computing, R Foundation for Statistical Computing, Vienna, Austria, https://www.R-project.org/, 2017.

Roberts, J.: Plants and water in forests and woodlands, pp. 181–236, Routledge, 1999.

Rosa, I. M., Smith, M. J., Wearn, O. R., Purves, D., and Ewers, R. M.: The Environmental Legacy of Modern Tropical Deforestation, Current Biology, 26, 2161–2166, https://doi.org/10.1016/j.cub.2016.06.013, http://www.sciencedirect.com/science/article/pii/S096098221630625X, 2016.

Sanford Jr., R. L., Paaby, P., Luvall, J. C., and Phillips, E.: Climate, geomorphology, and aquatic systems., in: La Selva. Ecology and natural history of a Neotropical Rainforest, edited by McDade, L. A., Bawa, K. S., Hespenheide, H. A., and Hartshorn, G. S., chap. 3, pp. 19–33, The University of Chicago Press, 1994.

Savenije, H. H. G.: The importance of interception and why we should delete the term evapotranspiration from our vocabulary, Hydrological Processes, 18, 1507–1511, https://doi.org/10.1002/hyp.5563, 2004.

Saxton, K. and Rawls, W.: Soil Water Characteristic Estimates by Texture and Organic Matter for Hydrologic Solutions, Soil Science Society of America journal, 70, 1569–1578, https://doi.org/10.2136/sssaj2005.0117, 2006.

Schellekens, J., Bruijnzeel, L. A., Scatena, F. N., Bink, N. J., and Holwerda, F.: Evaporation from a tropical rain forest, Luquillo Experimental Forest, eastern Puerto Rico, Water Resources Research, 36, 2183–2196, https://doi.org/10.1029/2000WR900074, 2000.

Shuttleworth, W.: Evaporation, in: Handbook of hydrology, edited by Maidment, D. R., chap. 4, pp. 4.1–4.53, Mc-Graw Hill, Inc., New York, 1993.

Sioris, C. E., Malo, A., McLinden, C. A., and D'Amours, R.: Direct injection of water vapor into the stratosphere by volcanic eruptions, Geophysical Research Letters, 43, 7694–7700, https://doi.org/10.1002/2016GL069918, 2016.

Sollins, P., Sancho M., F., Mata Ch., R., and Sanford Jr., R. L.: Soils and soil process research, in: La Selva. Ecology and natural history of a Neotropical Rainforest, edited by McDade, L. A., Bawa, K. S., Hespenheide, H. A., and Hartshorn, G. S., chap. 4, pp. 34–53, The University of Chicago Press, 1994.

Sparks, W. B., Richter, M., deWitt, C., Montiel, E., Russo, N. D., Grunsfeld, J. M., McGrath, M. A., Weaver, H., Hand, K. P., Bergeron, E., and Reach, W.: A Search for Water Vapor Plumes on Europa using SOFIA, The Astrophysical Journal, 871, L5, https://doi.org/10.3847/2041-8213/aafb0a, 2019.

Spellman, F. R.: The Handbook of Meteorology, Scarecrow Press, http://ebookcentral.proquest.com/lib/delft/detail.action?docID=1077405, 2012.

Strong, M., Sharp, Z. D., and Gutzler, D. S.: Diagnosing moisture transport using D/H ratios of water vapor, Geophysical Research Letters, 34, https://doi.org/10.1029/2006GL028307, 2007.

Stull, R. B.: An introduction to boundary layer meteorology, vol. 4, Springer Netherlands, Dordrecht, 1 edn., https://doi.org/10.1007/978-94-009-3027-8, 1988.

Stull, R. B.: Practical meteorology: an algebra based survey of atmospheric science, BC Campus, http://www.eos.ubc.ca/books/Practical_Meteorology/, 2016.

Tang, H., Dubayah, R., Swatantran, A., Hofton, M., Sheldon, S., Clark, D. B., and Blair, B.: Retrieval of vertical LAI profiles over tropical rain forests using waveform lidar at La Selva, Costa Rica, Remote Sensing of Environment, 124, 242 – 250, https://doi.org/10.1016/j.rse.2012.05.005, http://www.sciencedirect.com/science/article/pii/S0034425712002088, 2012.

Trzeciak, T. M., Garcia-Carreras, L., and Marsham, J. H.: Cross-Saharan transport of water vapor via recycled cold pool outflows from moist convection, Geophysical Research Letters, 44, 1554–1563, https://doi.org/10.1002/2016GL072108, 2017.

https://doi.org/10.5194/hess-2020-14
Preprint. Discussion started: 23 January 2020

van der Ent, R. J. and Savenije, H. H. G.: Length and time scales of atmospheric moisture recycling, Atmospheric Chemistry and Physics, 11, 1853–1863, https://doi.org/10.5194/acp-11-1853-2011, https://www.atmos-chem-phys.net/11/1853/2011/, 2011.

Wang, J., Krejci, R., Giangrande, S., Kuang, C., Barbosa, H. M. J., Brito, J., Carbone, S., Chi, X., Comstock, J., Ditas, F., Lavric, J., Manninen, H. E., Mei, F., Moran-Zuloaga, D., Pöhlker, C., Pöhlker, M. L., Saturno, J., Schmid, B., Souza, R. A. F., Springston, S. R., Tomlinson, J. M., Toto, T., Walter, D., Wimmer, D., Smith, J. N., Kulmala, M., Machado, L. A. T., Artaxo, P., Andreae, M. O., Petäjä, T., and Martin, S. T.: Amazon boundary layer aerosol concentration sustained by vertical transport during rainfall, Nature, 539, https://doi.org/10.1038/nature19819, 2016.

Wang, P. K.: Moisture plumes above thunderstorm anvils and their contributions to cross-tropopause transport of water vapor in midlatitudes, Journal of Geophysical Research: Atmospheres, 108, https://doi.org/10.1029/2002JD002581, 2003.

Wright, J. S., Fu, R., Worden, J. R., Chakraborty, S., Clinton, N. E., Risi, C., Sun, Y., and Yin, L.: Rainforest-initiated wet season onset over the southern Amazon, Proceedings of the National Academy of Sciences, 114, 8481–8486, https://doi.org/10.1073/pnas.1621516114, 2017.

https://doi.org/10.5194/hess-2020-14
Preprint. Discussion started: 23 January 2020

Hydrology and Earth System Sciences
Discussions
Open Access
EGU

Appendix A: Daily variables measured at the MRI–plot

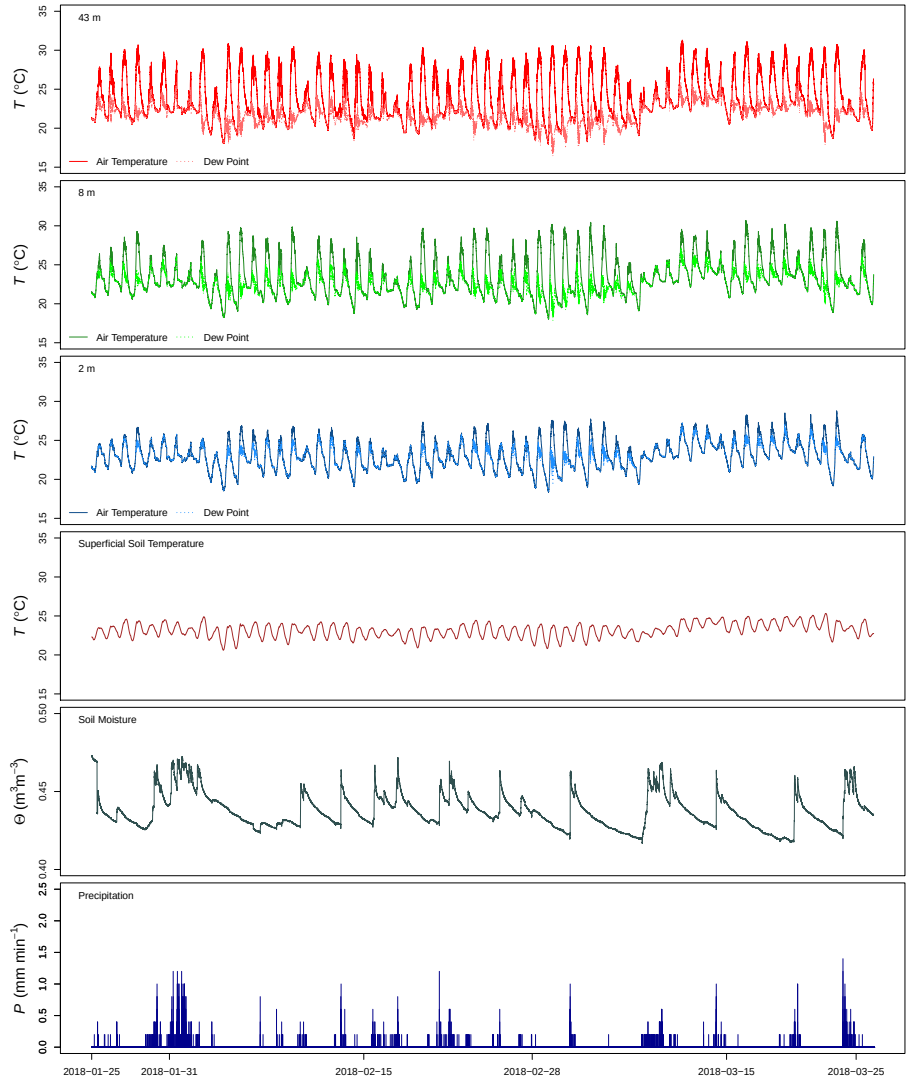

Figure A1. Detailed measurements performed at the MRI–plot between 2018-01-24 and 2018-03-26 along the canopy and within the soil.

https://doi.org/10.5194/hess-2020-14
Preprint. Discussion started: 23 January 2020

Hydrology and Earth System Sciences
Discussions

Appendix B: Time-lapse videos detailed information

Table B1. Sampling intervals and time frame of the 4 sampling days surveyed with the camera.

Sampling Date	Time Interval	Initial Time	Final Time
2018-03-21	5 minutes	11:27	17:45
2018-03-22	5 minutes	8:00	11:00
2018-03-22	1 minute	11:00	18:00
2018-03-23	1 minute	5:10	16:42
2018-03-24	1 minute	5:30	16:42
2018-03-25	1 minute	5:32	17:38

Note: the change of sampling intervals from 5 minutes to 1 minute was carried out the second day of video monitoring aiming to improve the quality of the survey.

https://doi.org/10.5194/hess-2020-14
Preprint. Discussion started: 23 January 2020

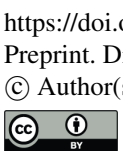

Hydrology and Earth System Sciences
Discussions
Open Access
EGU

Appendix C: Boxplots

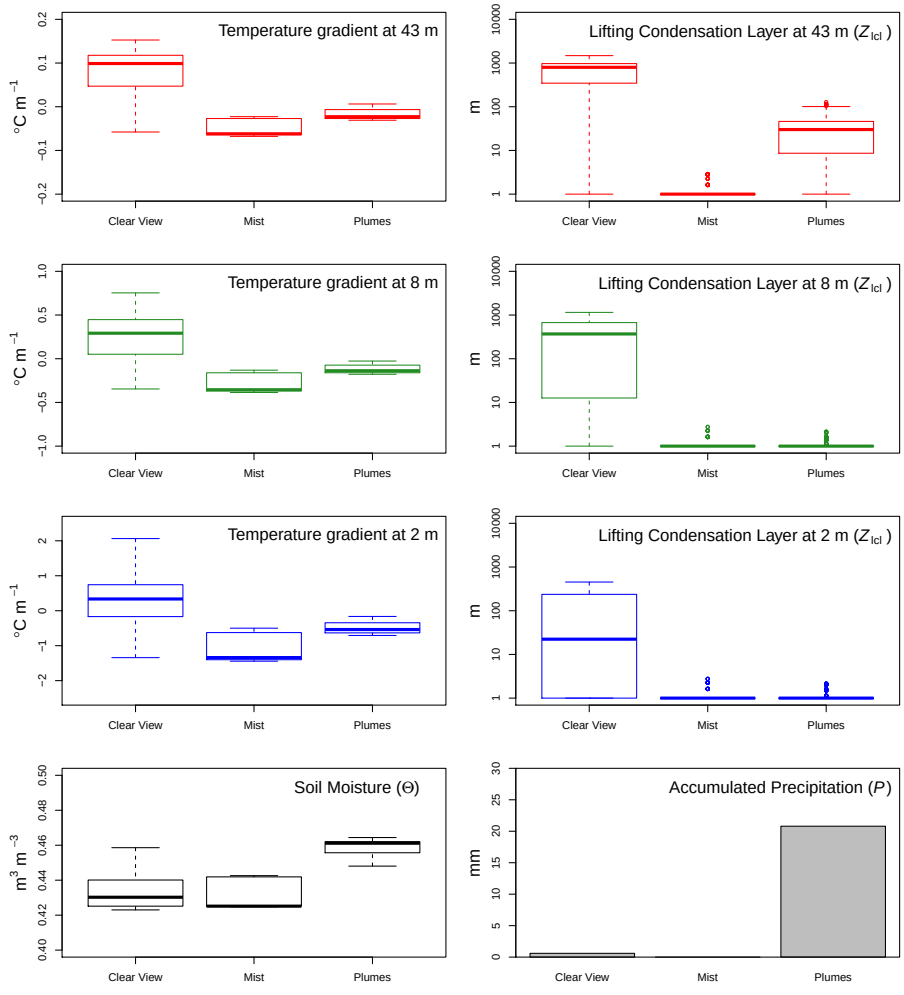

Figure C1. Boxplots describing the temperature gradients ($\frac{\Delta\theta_v}{\Delta z}$) and lifting condensation level (Z_{lcl}) at 43 m, 8 m and 2 m, as well as soil moisture (Θ) and total precipitation (P) of the three visual categories evaluated.